Journal of Hazardous Materials, 16 (1987) 427–438
Elsevier Science Publishers B.V., Amsterdam — Printed in The Netherlands

DEVELOPMENT AND APPLICATION OF HEAVY GAS DISPERSION MODELS OF VARYING COMPLEXITY

D.M. DEAVES

W.S. Atkins Engineering Sciences, Woodcote Grove, Ashley Road, Epsom, Surrey KT18 5BW (Great Britain)

(Received November 6, 1986; Accepted December 23, 1986)

Summary

The data which has been obtained from the Thorney Island trials has already been put to good use in model validation and development. This paper demonstrates how that data has been used to enhance a 'box' type model, and how comparisons between Phase I and Phase II results can suggest ways in which more complex mathematical modelling can be applied. Particular emphasis is placed on the manner in which each type of model is likely to be used during consequence analysis studies.

1. Introduction

The interest in heavy gas dispersion over the last few years has resulted in the development of a number of mathematical models, known as box models, which predict the integrated characteristics of a heavy gas cloud. These have been developed both for instantaneous releases [1] and for continuous releases [2], and a recent excellent review [3] has set out the theory of and comparisons between many of these models. A detailed analysis [4] of the Thorney Island Phase I results [5] has been used to develop a generalised Picknett-type model [6], with parameters optimised using the data, and has also produced general conclusions on the assumptions made in most box models.

The analysis presented in this paper re-examines certain of the assumptions of standard box models in the light of the data from Thorney Island. It also demonstrates how certain improvements can be introduced when the analytical solution, which is the basis for most box models, is replaced by a simple one-dimensional time integration (or distance integration, for a continuous release).

Whilst box models are generally adequate for dispersion over flat unobstructed terrain, more complex mathematical models [7] are required for a description of the effects of obstructions. Some comparisons between Phase II results have been used to demonstrate the different ways in which complex models can be used to assist in predicting the effects of such scenarios.

0304-3894/87/$03.50

2. Improvements to box models

The basic set of equations for box models of heavy gas dispersion are well known and documented [3] and will not be reproduced here. Differences between models occur in the formulation of entrainment parameters, cloud advection velocity, etc.

The integration of the differential equations which constitute the model can be undertaken either analytically, or numerically. Most modellers have preferred to use analytical techniques. However, certain simplifications are necessary in order that analytical solutions may be obtained. These include:

(a) the use of a particular formulation for the speed of the gravity current head, in which ρ_a, the density of air, appears in the denominator.

(b) the use of a cloud advection velocity which is imposed *after* integration of the equations, rather than one which accurately reflects the momentum balance.

(c) the requirement that any transition to passive dispersion should be sudden rather than gradual.

In the practical application of box models, they are frequently coded into computer programs for ease of use. If this is the case, then there is no particular reason to prefer an analytical solution, provided that an efficient algorithm can be used for the numerical integration.

Whilst simplification (a) above is not a significant disadvantage to the modelling of heavy gas dispersion, it is shown in the next section how relaxation of this requirement enables a more consistent formulation to be used for the 'slumping' velocity. Simplifications (b), and (c), however, do set serious limitations on the accuracy with which the models can cope with the following features:

(b): the initial stages of cloud acceleration

(c): the final stages of cloud lift-off.

Indications of improvements in both these areas are given below.

Formulation of slumping velocity

The velocity (u_f) of propagation of the cloud front is given by

$$u_f = \frac{dR}{dt} = c\left[\left(\frac{\rho - \rho_a}{\rho_r}\right)gh\right]^{\frac{1}{2}} \quad (1)$$

where R = radius of the cloud, c = constant, ρ_r = 'reference' density, and ρ_a = density of ambient air.

The definition of ρ_r depends upon the way in which eqn. (1) is derived, and can be set to either ρ_a, or ρ (the local value of cloud density). Picknett [6] and Fryer and Kaiser [1] have used $\rho_r = \rho_a$, while Van Ulden [8] has used $\rho_r = \rho$. In the latter case, values in the range $1 < c \leqslant \sqrt{2}$ have generally been used to fit the data.

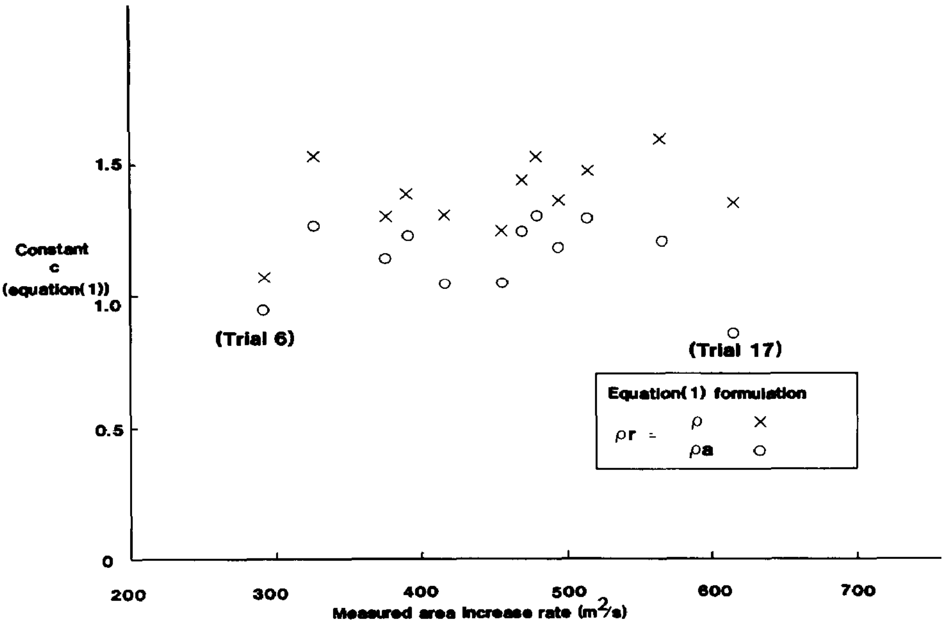

Fig. 1. Calculation of spreading rate constant.

It has been pointed out [9] that both the derivation and application of the formulation with $\rho_r = \rho_a$ are superior to those for $\rho_r = \rho$. In particular, $\rho_r = \rho_a$ enables certain analytical similarity solutions to be obtained for idealised inviscid flows with zero entrainment. However, use of numerical integration within a box model allows either formulation to be used, and two versions of the Atkins ES program SLUMP have therefore been developed for comparison of model results, and to enable that form of u_f which best fits the Thorney Island Phase I data to be incorporated.

Where the initial density ratio is near 1, there is little to choose between the two models. However, differences become more marked for higher density ratios, and the best formulation will be that which provides the most consistent value of the spreading constant c over the widest range of density ratios.

The propagation velocity u_f can best be ascertained from the initial area increase rate, as measured before any transition to passive dispersion occurs. This is independent of both the advection velocity, and also the other model parameters α and β. Both versions of the model were run using $c = 1$; the ratio of the measured area increase rate (as estimated by Brighton et al. [10]) to that computed by the model then gives the best value of c for that model. Results are shown in Fig. 1 for a representative sample of Phase I trials.

Trials 5 and 12 were not included, because of defects in the release system, and overhead photography, respectively. Of the remainder, Trials 6, 13 and 17

TABLE 1

Mean values (and % standard deviation) of constants c in eqn. (1)

Trials	$\rho_r=\rho_a$	$\rho_r=\rho$
ALL	1.15 (12)	1.38 (10)
ALL−6	1.17 (11)	1.41 (7.7)
ALL−(6,13,17)	1.19 (7.4)	1.41 (8.2)

were quoted, by Brighton et al. [10], as having a significant portion of the cloud not visible. This is unfortunate, since Trial 17 was the only one for which the initial density ratio (4.2) was significantly greater than 2, and therefore should be useful in identifying which of the two formulations is best. Trial 6 showed a much lower cloud increase rate than other comparable trials, and the estimated increase is therefore slightly suspect.

Taking these features of the trials into account, the means and standard deviations of those trials considered are summarised in Table 1 for: (a) all Phase I trials considered (ALL), (b) all except Trial 6 (ALL-6), and (c) all except Trials 6, 13, 17 (ALL−(6,13,17)). Standard deviations (as a percentage of the mean) are given in brackets.

Although these results do not conclusively demonstrate which formulation is superior, it appears that $\rho_r=\rho$ generally shows less scatter, giving a value of $c=\sqrt{2}$. This particular formulation also appears to be more consistent over a wide range of density differences (i.e. to include Trial 17).

Cloud advection

A serious shortcoming of analytically integrated box models is that the velocity of the cloud, and hence its position, has to be specified independently of the slumping process. Numerical integration of the model equations, however, enables the local cloud velocity to be calculated on the basis of the initial momentum of the cloud (usually zero for an instantaneous release), and the momentum of the entrained air.

The computer program SLUMP has therefore been developed to provide a more realistic estimate of cloud advection in the instantaneous release case. The initial inertia of the cloud is included, and the resultant equations are, for cloud positions at time step j:

$$m_j = m_{j-1} + \rho_a \frac{\mathrm{d}V}{\mathrm{d}t} \Delta t \tag{2}$$

$$M_j = M_{j-1} + (m_j - m_{j-1}) u_r \tag{3}$$

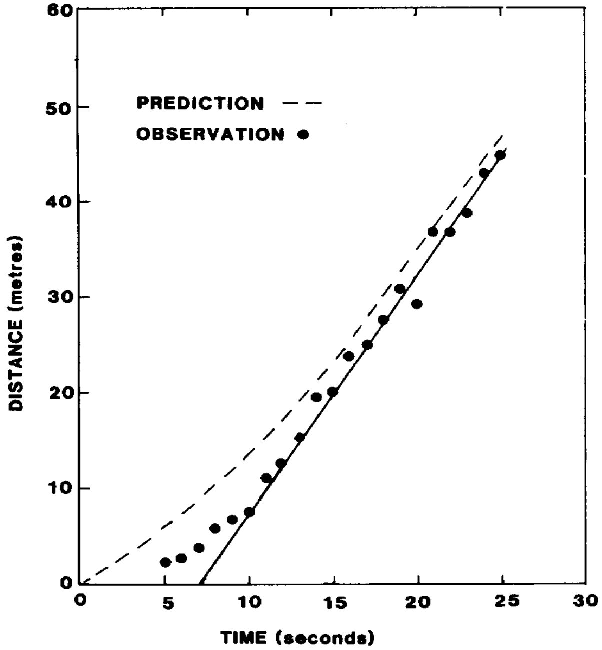

Fig. 2. Prediction of cloud acceleration for Trial 14 and comparison with observations.

$$u_r = \frac{u_*}{k} \ln\left(\frac{h_{j-1}}{2z_0}\right) \tag{4}$$

where m_j = mass of cloud at time step j, M_j = momentum of cloud at time step j, u_* = friction velocity of ambient wind, u_r = reference velocity of entrained air at time step j, z_0 = roughness length of ground surface, k = von Karman's constant (= 0.4), and $(\mathrm{d}V/\mathrm{d}t)\Delta t$ is the cloud volume increase over timestep Δt due to the normal top and side entrainment processes.

The velocity of the cloud (u_j) at time step j can then be deduced from the total mass and momentum within the cloud:

$$u_j = M_j / m_j \tag{5}$$

and this can be used to estimate the position of the cloud centre.

Other authors [11] have considered cloud advection in more detail, and, in particular, have examined the effects of drag on the far downwind advection. It is acknowledged that the formulation given in eqn. (4) above is perhaps the simplest which could be used, and is applicable primarily in the near field.

Figure 2 shows a comparison of computed centroid position with those deduced by Brighton et al. [10] for Thorney Island Trial 14. The agreement is generally good except in the earliest stages of cloud development. However, the concave shape of the curve indicates that the initial cloud acceleration is now being modelled at least qualitatively correctly. In contrast, use of a fixed proportion of a reference ambient windspeed would give a straight line through the origin, whilst use of the windspeed at a fixed fraction of the cloud height would give a convex curve, due to the decreasing height (and hence speed) in the initial stages of the cloud development.

Transition to passive dispersion

As the cloud becomes more diluted, so gravity effects become less significant, and passive dispersion takes over. The parameter which determines this change-over is the ratio of turbulence energy in the atmosphere to potential energy in the cloud

$$\gamma = \min\left[\left(\frac{u_*}{u_f}\right)^2, 1\right] \qquad (6)$$

where u_* and u_f are defined above.

It has been suggested [8] that the dispersion is essentially passive for $\gamma = 1$, whereas it will be gravity driven when $\gamma \ll 1$. Consequently, the rate of spreading, both in the vertical and horizontal direction, is taken as

$$\frac{d\phi}{dt} = (1-\gamma)\frac{d\phi_G}{dt} + \gamma\frac{d\phi_P}{dt} \qquad (7)$$

where ϕ is the actual cloud dimension and the subscripts G, P denote the appropriate gravity and passive dispersion values, respectively. The vertical and lateral dimensions of a passive cloud are estimated from the σ_y, σ_z values given by Smith [12]. These σ_y, σ_z values are given by

$$\begin{aligned} \sigma_y &= c_{1y} x^{c2y} \\ \sigma_z &= c_{1z} x^{c2z} \end{aligned} \qquad (8)$$

where values of the constants c_{1y}, c_{2y} etc. for instantaneous releases are dependent on stability class.

Predictions for the Phase I Trial 7 have been undertaken with and without the transition to passive dispersion. This trial was reported as having been carried out in stability class E. The SLUMP runs were therefore performed for both neutral and stable categories and the results shown in Fig. 3.

When comparing these predictions with the measurements, it should be noted that the predictions are for positions on the centre-line, whereas most of the measurements were off this line, and are therefore expected to be lower. Differences between the neutral stability predictions, and those for gravity driven dispersion are only small for most of the range considered, with the stable results showing consistently higher concentrations throughout. It would appear that the range of distances for which comparisons have been made is insuffi-

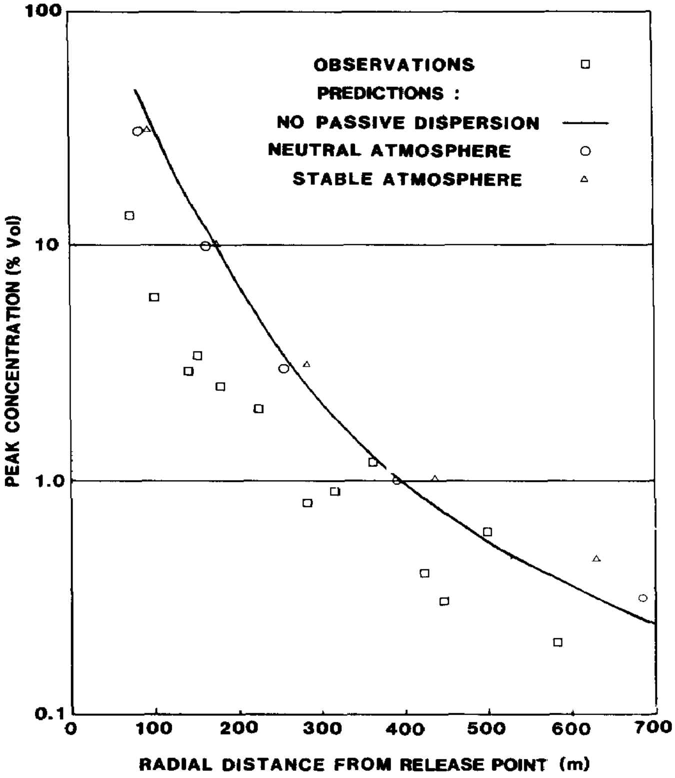

Fig. 3. Peak concentration as a function of distance from release point in Trial 7.

cient for any conclusions to be drawn about the effectiveness of the proposed transition to passive dispersion. However, the results do also suggest that the usual passive dispersion parameters, which are generally applied to heights in excess of 10 m for stack dispersion etc. may not be applicable to the lift-off phase of a dense gas at ground level.

3. Use of complex models

Box models have been developed and validated for the dispersion of releases of heavy gas in level, unobstructed terrain. When significant obstructions are present, as in the Phase II trials, box models are unable to describe the detail of the dispersion in the vicinity of such obstructions. The alternative for such situations is a full 3D solution of the Navier–Stokes equations in which atmospheric turbulence and its interaction with the dense cloud is modelled. Results of such a model have already been presented [7] as predictions for Trial 29 of Phase II.

The trials in which obstructions had the greatest effect on dispersion were those in which a solid 5 m fence was placed 50 m downwind of the source. In particular, run 21 was undertaken in very similar atmospheric conditions to run 7, and a comparison of peak concentrations between these two runs has been given [5]. It was the purpose of the brief study described on this section to use these comparisons to determine whether useful results could be produced using two-dimensional modelling, with its obvious savings in cost, data preparation time etc.

The Atkins ES program HEAVYGAS [13] can be used either in its fully 3D form [7], as indicated above, or in a 2D plane or axisymmetric form. The configuration of Trial 21 apparently could be modelled well using the axisymmetric form. However, the axis of symmetry has to lie on the axis of the heavy gas cylinder, and this is only possible when there is no wind. Although a 2D plane solution does not allow out-of-plane mixing, it does allow for a non-zero windspeed.

The following two runs were therefore undertaken:

(a) axisymmetric run with zero windspeed

(b) plane run with windspeed 3.9 m/s and source scaled down to allow for effects of out-of-plane mixing.

Results for peak centre-line concentration are shown in Fig. 4, where they are compared with the measurements of Trial 21.

Both sets of results show the significant fall in concentration across the fence. The rather large change predicted by the axisymmetric run is due to the lack of ambient windspeed to carry the dense gas over the fence; the region within the fence tends to fill up, and only slowly overtop the fence. The rather small change predicted by the plane run can be accounted for by the fact that the fence in reality spreads the gas sideways, rather than just allowing it to overtop in one vertical plane.

The mass of gas released at the source has been scaled down by a factor of 50, on the assumption that the lateral spread of the cloud is of order 50 m at the fence position. This reduction in source size has considerably reduced the effects of the high density of the cloud, and, in particular, has allowed rather more vertical dispersion than happens in practice. In order to improve on these results, some upward adjustment of the source would be necessary to ensure that concentrations are matched just upwind of the fence.

2D or 3D flow models, of which HEAVYGAS is an example, also provide information about both the flow field, and also the concentration profiles within the cloud. Examples of these predicted profiles are given in Figs. 5 and 6, and enable further interesting comparisons to be made betweenthe two simulations, and also between predictions and measurements.

Figure 5 shows the peak concentration profiles predicted and measured downwind of the fence. It can be seen that the profile shape is most closely modelled by the plane simulation, although the position of the peak concentration, at just above fence height, is rather under-estimated. It is suggested

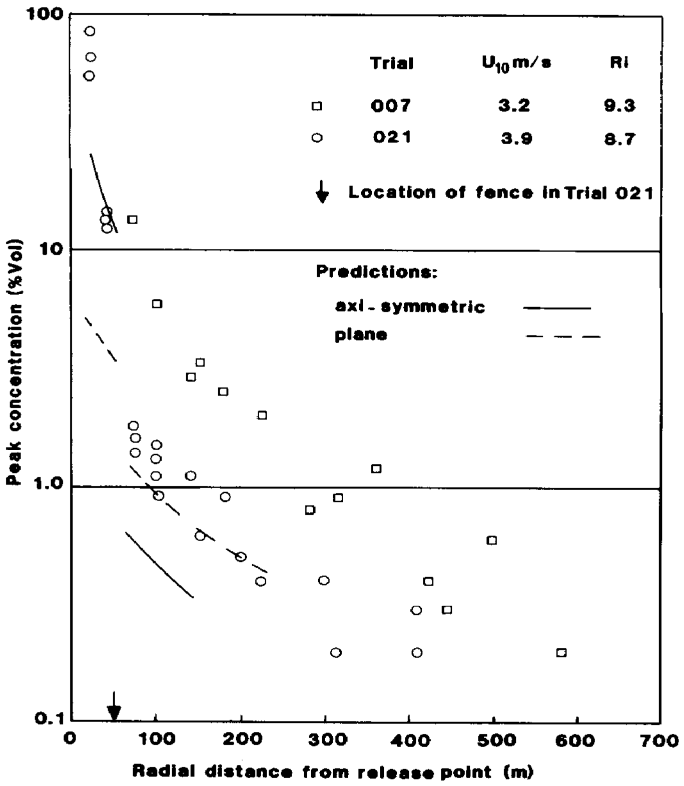

Fig. 4. 2D model predictions for Trial 21.

that this is due to the necessary scaling of the source, which has actually reduced the density effects, and in particular the observed 'splashing' over the fence. As indicated above, the axisymmetric results show the effects of the dense gas cloud gently spilling over the fence, rather than being blown over it.

Figure 6 shows, for the plane simulation only, the development, during the time of passage of the cloud, of the concentration profile 25 m downwind of the fence. Although it is only compared with the profile of measured peak values, it does serve to demonstrate the stages in the cloud development at this point:

(a) 10 s — cloud has just overtopped the fence, sending a 'jet' of higher concentration over the height range 5–10 m.

(b) 34 s — bulk of cloud has now overtopped the fence, filling out the lower portion of the profile, and reducing the height of the maximum to about 6 m.

(c) 100 s — effects of fence on profile at this particular location have virtually disappeared.

A final example of the information obtained from these simulations is shown in Fig. 7. In this case, the results from Brighton and Prince's [14] analysis of

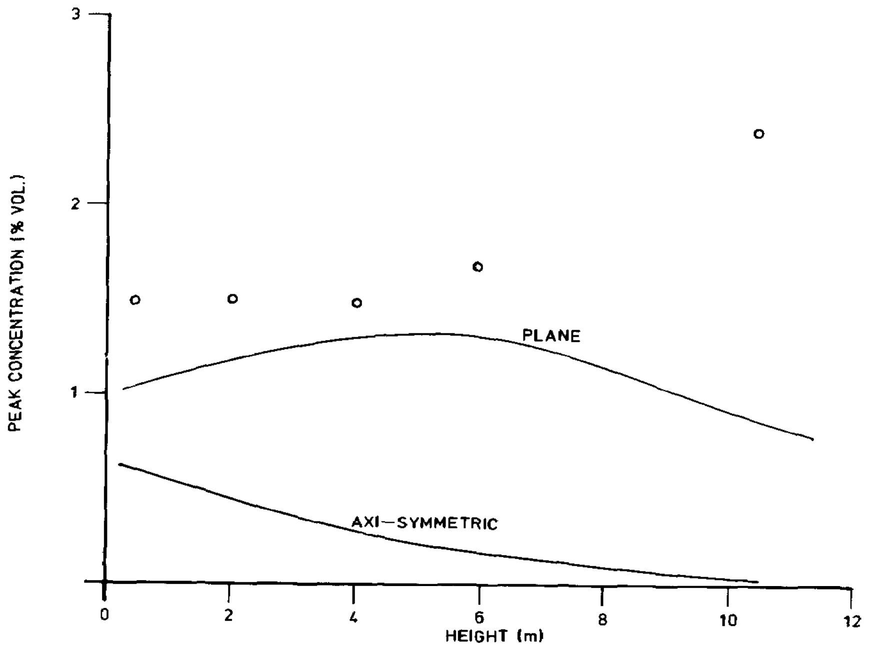

Fig. 5. Predicted profiles of peak concentration versus height at 25 m downwind of the impermeable fence in Trial 21.

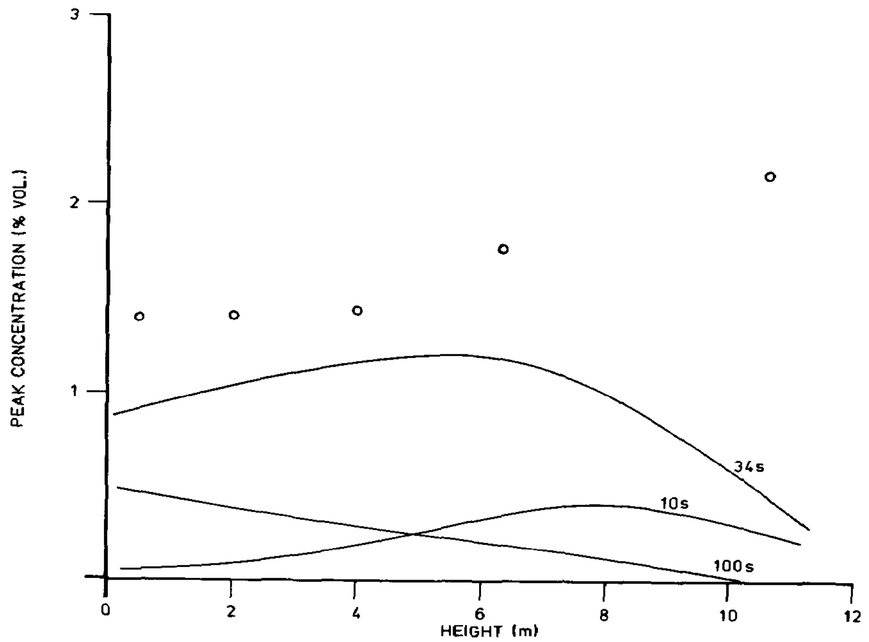

Fig. 6. Development of concentration profiles downwind of fence in Trial 21; predictions using plane geometry.

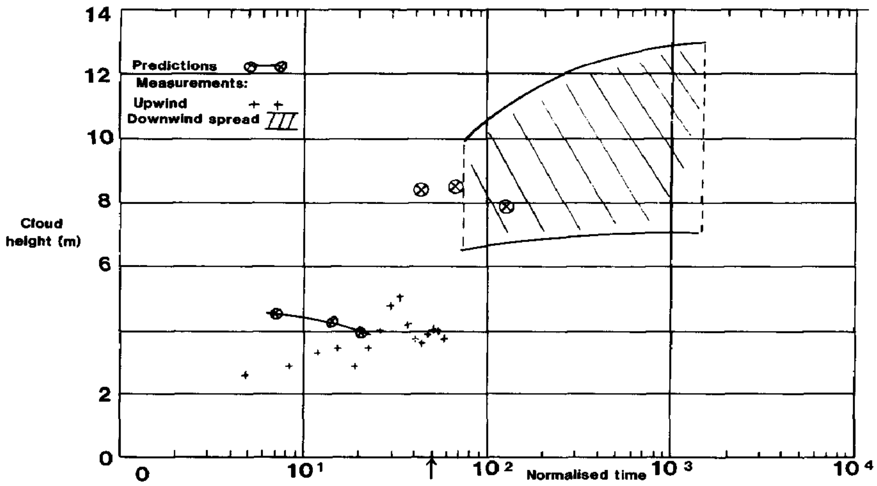

Fig. 7. Comparison of cloud height predictions and measurements for Trial 21.

Trial 21 have been slightly simplified, and compared with model results, this time from the axisymmetric simulation. Cloud height, defined as height to 10% of mean ground level concentration, is plotted against non-dimensionalised time. The comparison is reasonably good, indicating that, in this case, axisymmetric modelling predicts the cloud height increase quite well, and hence could be used to assess effects immediately upwind of the fence.

In spite of the obvious limitations of the results of 2D modelling presented here, it is evident that they can be used to give at least an order-of-magnitude indication of the effects of obstructions. In this case, the results have effectively given upper and lower bounds on the downwind concentrations, and could therefore be used, with some caution and considerable judgment, in assessing the effects of obstructions on gas dispersion. More highly 3D flows, such as those around roughly cubical buildings, are rather less amenable to a 2D analysis of this type, and may, in certain circumstances, justify the use of a fully 3D model.

4. Conclusions

Simple box models

It has been shown how the use of analytical integration enables the following features to be incorporated into a standard box model:

— use of more realistic form of spreading velocity

— incorporation of cloud inertia effects

— gradual transition to passive dispersion.

In each case, data from Phase I has been used for the validation and justification of the improvements made. However, within the range of the observations, there appears to be insufficient evidence to ascertain whether the modelling of the transition to passive dispersion is adequate. Whilst this inadequacy is not a serious limitation for flammable gas dispersion, it is important that this area should be improved for toxic gas releases, in which concentrations are significant down to a few parts per million.

Use of complex models

A particular example has been presented, based upon one of the Phase II trials, in order to demonstrate how 2D versions of the more complex flow-field models can be used to determine the effects of obstructions. It is concluded that, provided the limitations of such an approach are understood, there will be certain classes of problems for which the effects of obstructions can be predicted using relatively inexpensive and flexible 2D modelling. Evidently, the possibility of 3D modelling [7] exists for improved estimates in such situations, but it is envisaged that there will be very few cases in which its expense could be justified.

References

1 L.S. Fryer and G.D. Kaiser, DENZ, a computer program for the calculation of the dispersion of dense toxic or explosive gases in the atmosphere, Report No. SRD R152, Safety and Reliability Directorate, UKAEA, Culcheth, UK, 1979.
2 S.F. Jagger, Development of CRUNCH: a dispersion model for continuous releases of a denser-than-air vapour into the atmosphere, Report No. SRD R229, Safety and Reliability Directorate, UKAEA, Culcheth, UK, 1983.
3 C.J. Wheatley and D.M. Webber, Aspects of the dispersion of denser-than-air vapours relevant to gas cloud explosions, Report No. EUR 9592, Commission of the European Communities, Brussels, 1984.
4 C.J. Wheatley, A.J. Prince and P.W.M. Brighton, Comparison between data from the Thorney Island Heavy Gas Trials and predictions of simple dispersion models, Report No. SRD R355, Safety and Reliability Directorate, UKAEA, Culcheth, UK, 1986.
5 J. McQuaid and B. Roebuck, Large scale field trials on dense vapour dispersion, Report No. EUR 10029, Commission of the European Communities, Brussels, 1985.
6 R.G. Picknett, Dispersion of dense gas puffs released in the atmosphere at ground level, Atmos. Environ., 15 (1981) 509–525.
7 D.M. Deaves, 3-Dimensional model predictions for the upwind building trial of Thorney Island Phase II, J. Hazardous Materials, 11 (1985) 341–346.
8 A.P. van Ulden, On the spreading of a heavy gas cloud released near the ground. In: Proc. 1st Int. Loss Prevention Symposium, The Hague, 1974.
9 D.M. Webber, Personal communication, 1986.
10 P.W.M. Brighton, A.J. Prince and D.M. Webber, Determination of cloud area and path from visual and concentration records, J. Hazardous Materials, 11 (1985) 155–178.
11 C.J. Wheatley and A.J. Prince, Translational cloud speeds in the Thorney Island trials: Mathematical modelling and data analysis, J. Hazardous Materials, 16 (1987) 185–199.
12 F.B. Smith, A scheme for estimating the vertical dispersion of a plume from a source near ground level, In: Proc. 3rd Meeting of an Expert Panel on Air Pollution Modelling, Paris, October 1972, Brussels, NATO-CCMS Report 14, 1972.
13 D.M. Deaves, Application of a turbulence flow model to heavy gas dispersion in complex situations, In: S. Hartwig (Ed.), Heavy Gas and Risk Assessment II, Reidel, Dordrecht, 1983.
14 P.W.M. Brighton and A.J. Prince, Overall properties of the heavy gas clouds in the Thorney Island Phase II trials, J. Hazardous Materials, 16 (1987) 103–138.